Initial Disulfide Formation Steps in the Folding of an ω-Conotoxin†

Marian Price-Carter, Grzegorz Bulaj, and David P. Goldenberg*

Department of Biology, University of Utah, 257 South 1400 East, Salt Lake City, Utah 84112-0840

Received November 8, 2001; Revised Manuscript Received January 18, 2002

ABSTRACT: To determine whether the native disulfides of ω-conotoxins are preferentially stabilized early in the folding of these small proteins, the rates and equilibria for disulfide formation were measured for three analogues of ω-conotoxin MVIIA. In each analogue, one of the three pairs of disulfide-bonded Cys residues was replaced with Ala residues, leaving four Cys residues that can form six intermediates with one disulfide and three species with two disulfides. For each analogue, all of the disulfide-bonded species were identified, and the equilibrium constants for forming the individual species via exchange with oxidized and reduced glutathione were measured. These equilibrium constants represent effective concentrations of the Cys thiols and ranged from 0.01 to 0.4 M in the fully reduced protein. There was little or no preference for forming the native disulfides, and the equilibria for forming the first and second disulfides decreased only slightly upon the addition of 8 M urea. The data for the four-Cys analogues, together with equilibrium data for the six-Cys form, were also used to estimate effective concentrations for forming a third disulfide once two native disulfides are present. These effective concentrations were approximately 100 and 10 M in the presence of 0 and 8 M urea, respectively. The results indicate that there is little or no preferential formation of native interactions in the folding of these molecules until two disulfides have formed, after which there is a high degree of cooperativity among the native interactions.

The ω-conotoxins are small disulfide-bonded polypeptides that are found in the venoms of carnivorous marine snails of the genus *Conus*, and the toxins act to block presynaptic voltage-gated Ca^{2+}-channels in the snails' prey, thus contributing to the potent paralytic activities of these venoms (*1*). Over 60 ω-conotoxin sequences have been identified, and these moleules display considerable specificity for Ca^{2+}-channel subtypes, making them especially valuable reagents for neurobiology research. They are also being actively pursued as potential pharmaceuticals, and the subject of the current study, ω-MVIIA,[1] has shown promise for the treatment of chronic pain (*2, 3*). (Synthetic ω-MVIIA is also known as SNX-111 and by the drug name ziconotide.)

Although they are only 25−30 amino acid residues long, the ω-conotoxins fold into well-defined three-dimensional structures that are stabilized by three conserved disulfide bonds. Their overall folds are also conserved (*4*−*7*) and are representative of a motif, described as a "knottin" or "inhibitory cysteine knot" (ICK), that has been found in numerous small proteins derived from remarkably diverse sources (*8*−*10*). In addition to the three disulfides, the motif is characterized by the presence of a β-sheet composed of three short strands (Figure 1). While the pattern of disulfides and secondary structure are conserved among the ω-conotoxins, their sequences show little or no conservation other than that of the Cys residues.

The small size and limited sequence conservation seen in the ω-conotoxins and other proteins with the ICK fold raise fascinating questions about the folding mechanisms of these molecules. While the disulfide bonds play a critical role in stabilizing the fold (*11, 12*), these disulfides must form correctly after the chain is synthesized. Like other peptides found in *Conus* venoms, the ω-conotoxins are synthesized as larger precursors, and it was initially suggested that an N-terminal pro-peptide might play a role in directing folding (*13, 14*). It has been found, however, that the mature sequences can refold and form their disulfides with modest efficiency, ranging from 20 to 80%, after being fully reduced, as compared to 5−10% expected if the disulfides were to form randomly (*15*). In the case of ω-MVIIA, it was further shown that the propeptide sequence actually decreases slightly the folding efficiency in vitro (*16*).

The ω-conotoxins are also synthesized with an extra C-terminal Gly residue, which is oxidatively cleaved to create an amidated C-terminus. A form of ω-MVIIA with this Gly residue is about 1 kcal/mol more stable than the mature amidated form and refolds with an efficiency greater than 80%, versus 50% for the mature peptide (*16*). An NMR-derived solution structure of the Gly containing form,

† Supported by NSF Grant MCB-9316065 and NIH Grant GM42594. Peptide synthesis and mass spectroscopy services were supported by National Cancer Institute Grant 5 P30 CA 42014 and the Huntsman Cancer Institute. M.P-C. was the recipient of a postdoctoral fellowship from the Markey Center for Protein Biophysics at the University of Utah.

* Corresponding author. E-mail: goldenberg@biology.utah.edu.

[1] Abbreviations: ω-MVIIA-Gly, a form of ω-conotoxin MVIIA composed of the mature sequence plus a C-terminal Gly residue with an unmodified carboxyl group; ICK, inhibitor cysteine knot; 1,16Ala, 8,20Ala, and 15,25Ala are analogues of ω-MVIIA-Gly with the indicated Cys residues replaced with Ala. Forms of the analogues with specific disulfide bonds are indicated by the numbers of the disulfide-linked Cys residues, enclosed in brackets and followed by a subscript indicating the analogue. Thus, $[8-20,15-25]_{1,16Ala}$ is the form in which Cys 1 and 16 are replaced with Ala, and the other four-Cys residues are disulfide bonded as in the native structure; GSSG and GSH, the disulfide and thiol forms, respectively, of glutathione; DTT, dithiothreitol; MOPS, 3-(*N*-morpholino)propanesulfonic acid; EDTA, ethylenediaminetetraacetic acid; TFA, trifluoroacetic acid; TCEP, tris(2-carboxyethyl)phosphine; CDAP, 1-cyano-4-(dimethylamino)-pyridinium tetrafluoroborate; HPLC, high performance liquid chromatography.

10.1021/bi012033c CCC: $22.00
Published on Web 02/12/2002

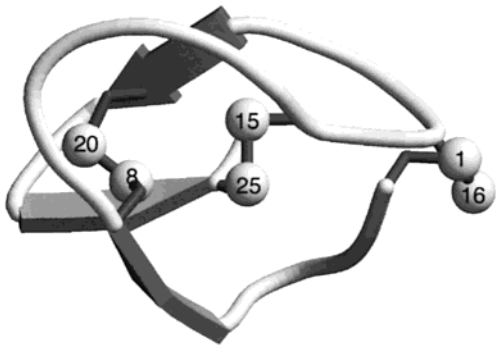

FIGURE 1: Native structure of ω-MVIIA-Gly. The ribbon diagram was drawn using the atomic coordinates determined by solution NMR spectroscopy (*17*). The disulfide bonded sulfur atoms are represented as balls with the Cys residue numbers indicated. The figure was drawn with the programs MOLSCRIPT and Raster3d (*54*, *55*), using the atomic coordinates of molecule number 9 (the structure with the smallest RMS deviation from the calculated mean structure) in entry 1FEO of the Protein Data Bank.

designated ω-MVIIA-Gly, indicates that it has a folded conformation very similar to that of the mature form and that the C-terminal Gly residue forms a network of hydrogen bonds that likely contribute to its stability (*17*). Since oxidation of the Gly residue is thought to take place in secretory granules following folding and disulfide formation (*18*), these extra interactions may be quite significant for folding in vivo. We have thus adopted ω-MVIIA-Gly as a model for studying the mechanism of folding and disulfide formation in this class of proteins.

To assess the roles of the individual disulfide bonds in folding, we previously prepared a set of three analogues, each with one pair of disulfide-bonded Cys residues replaced with Ala (*11*). Removing any one of the three disulfides was found to greatly decrease the affinity of the peptide for Ca^{2+}-channels, by 100- to 10 000-fold, and circular dichroism spectroscopy indicated that the β-sheet structures are destabilized. Furthermore, none of the three analogues form their correct disulfides as efficiently as ω-MVIIA-Gly with all six Cys residues, indicating that each disulfide plays an important role in stabilizing the other two.

In the present study, we have examined the four-Cys analogues more extensively, identifying each of the one-disulfide intermediates in their folding and determining the equilibrium constants for forming each of the possible species with one or two disulfide bonds. The results indicate that there is little or no conformational specificity that favors forming the first or second disulfide, but that any pair of native disulfides greatly favors formation of the third. It thus appears that the cooperativity in the folding of this small protein is expressed only when the chain is already significantly constrained.

EXPERIMENTAL PROCEDURES

Synthetic Peptides. Chemical synthesis of the three ω-MVIIA-Gly analogues used for these studies has been described previously (*11*). In each peptide, one of the Cys pairs that forms a disulfide in the native protein was replaced with Ala residues. The species with the native disulfides were generated by a selective protection−deprotection scheme (*11*). Samples of these forms were then reduced and allowed to form disulfides under conditions of reversible thiol-disulfide exchange, thus generating, for each analogue, all three of the possible forms with two disulfides. The identities of these species were determined previously by peptide mapping (*11*). ω-MVIIA-Gly with all three disulfides was prepared as described (*16*).

Identification of One-Disulfide Forms. To generate all of the possible one-disulfide forms of each four-Cys analogue, the purified two-disulfide forms, with native or non-native disulfides, were partially reduced with tris(2-carboxyethyl)-phosphine (TCEP, Pierce) at pH 3.0 (*19*). The resulting one-disulfide forms were purified by HPLC, lyophilized, and stored at −20 °C.

The free thiols in the partially reduced analogues were identified using the cyanylation-cleavage procedure described by Wu and Watson (*20*). Fresh solutions of 1-cyano-4-(dimethylamino)-pyridinium tetrafluoroborate (CDAP, Sigma), were prepared by dissolving the dry reagent in 0.17 M Na_3-citrate/PO_4 pH 3.0 to a concentration of 20 mM. The solutions were stored on ice in brown glass vials and used the same day. To cyanylate the free thiols in a conotoxin analogue, partially reduced peptide (resuspended in 0.17 M citrate pH 3.0) was incubated with CDAP in citrate buffer at 25 °C. The final free thiol concentration was 40 μM, and the final CDAP concentration 2 mM. After 20 min, the reaction mixtures were fractionated by reversed-phase HPLC. Completion of the cyanylation reaction was confirmed by electrospray ionization mass spectrometry, and the purified products were lyophilized and stored at −20 °C.

Peptide bonds preceding the cyanylated Cys residues were cleaved by mixing the modified peptides (resuspended at a concentration of 200 μM in 0.1% TFA) with 9 volumes of NH_4OH (0.02−1 M) and incubating for 5−20 min at 25 °C. The reactions were quenched by adding 0.1 volume of concentrated H_3PO_4, and the major products were purified by HPLC and analyzed by electrospray-ionization mass spectrometry. To resolve a few ambiguities in the assignments, some of the peptide was further digested with trypsin, and the resulting fragments were analyzed by mass spectrometry.

Disulfide Formation and Rearrangement Kinetics. Disulfide formation experiments were initiated by mixing a solution of fully reduced peptide in 10 mM HCl with an equal volume of refolding buffer mix to yield final concentrations of 20 μM peptide, 0.1 M MOPS−NaOH, pH 7.3, 0.2 M KCl, 1 mM EDTA and oxidized and reduced glutathione (GSSG and GSH) at concentrations appropriate for the experiment. To study the rearrangements of the one-disulfide species, the purified intermediates were resuspended in 10 mM HCl to a final concentration of 200 μM and then mixed with 9 volumes of a buffer solution to generate the same reagent concentrations as used in the disulfide formation experiments, except that no GSSG or GSH was added. All of the solutions were flushed with N_2, and the reactions were carried out in septum vials under an N_2 atmosphere. At various times after initiating the reactions, samples were withdrawn and quenched with 0.05 volumes of H_3PO_4.

After trapping by acidification, the various disulfide-bonded forms were fractionated by reversed-phase HPLC using buffer systems optimized for each analogue as described previously (*11*). For most separations, a Vydac C_{18} column was used and eluted with a gradient of acetonitrile in 0.1% TFA. For the 15,25Ala analogue, however, a Beckman C_{18} column was used to separate the reduction

products, and a Vydac diphenyl column was used to separate the different forms of 1,16Ala generated during disulfide rearrangement. The diphenyl column was eluted with a gradient of acetonitrile in 0.5% TFA, and the chromatography was carried out with the column in a 37 °C water bath. Elution profiles were monitored by absorbance at 220 nm (C_{18}) or 229 nm (diphenyl chromatography).

To analyze the kinetics of disulfide formation, the HPLC peaks corresponding to the various species were integrated, and the observed relative concentrations were compared to those predicted by numerical simulations based on the kinetic models described in the results and discussion section. For each four-Cys analogue, the rate constants making up the model were manually adjusted until a single set of constants accounted for all of the experiments utilizing different concentrations of GSSG and GSH.

Disulfide-Coupled Folding Equilibrium for ω-MVIIA-Gly. To measure the overall equilibrium constant for forming the three native disulfides in ω-MVIIA-Gly by exchange with glutathione, the native peptide was incubated with GSSG and GSH at 25 °C in the presence of 0.1 M MOPS−NaOH, pH 7.3, 0.2 M KCl, and 1 mM EDTA. Four experiments were carried out using GSSG:GSH concentrations of 0.5 mM:20 mM, 0.5 mM:30 mM, 1 mM:20 mM, and 1 mM:30 mM. A parallel set of measurements were carried out in the presence of 8 M urea, using 1 mM GSSG and 13, 16, or 20 mM GSH. The reactions were quenched after 2 h by acidification and analyzed by HPLC as described above. [Previous experiments demonstrated that equilibration of these reaction is reached in 2 h or less (*16*).] The relative concentrations of the native and fully reduced forms were determined by integration of the HPLC chromatograms, and the data were plotted in the form of the fraction native (f_n) as a function of the quantity $[GSH]^2/[GSSG]$. The data were fit by the method of least squares to the equation:

$$f_n = \frac{[N]}{[N] + [R]} = \frac{1}{1 + (1/K_{III})([GSH]^2/[GSSG])^3} \quad (1)$$

where K_{III} is the equilibrium constant, with units M^3. Uncertainties in the estimates of K_{III} were derived from the least-squares fit.

RESULTS AND DISCUSSION

A polypeptide containing six Cys residues can, in principle, form a total of 15 species with a single disulfide, 45 species with two disulfides, and 15 three-disulfide forms. During the folding of some disulfide-bonded proteins, such as bovine pancreatic trypsin inhibitor, only a relatively small subset of these species actually accumulate to significant levels, greatly simplifying the task of defining the major pathways of disulfide formation (*21*−*23*). For other proteins, however, there is a much broader distribution of disulfide-bonded species, making it much more difficult to identify any conformational tendencies of the polypeptide to favor particular disulfides (*24*−*26*). To test for the presence of such tendencies in the formation of the one- and two-disulfide intermediates in the folding of ω-MVIIA-Gly, we have used three synthetic analogues, each with one pair of Cys residues replaced with Ala. These three peptides (designated 1,16Ala, 8,20Ala, and 15,25Ala) can collectively form all 15 of the one-disulfide species of the unmodified peptide, as well as nine two-disulfide forms. In a previous study, we isolated and identified the three two-disulfide forms of each analogue and measured the equilibrium constants for the formation of these species from the fully reduced peptides (*11*). We have now isolated the six one-disulfide forms of each analogue, identified the disulfides by peptide mapping, and measured the tendencies of these disulfides to form via thiol disulfide exchange with glutathione.

Purification and Identification of One-Disulfide Forms. To identify all of the possible one-disulfide forms of ω-MVIIA-Gly, we generated each of these species by partially reducing the purified two-disulfide forms of each four-Cys analogue. The two-disulfide forms were selectively reduced with TCEP at pH 3.0, and the resulting products were purified by reversed-phase HPLC at low pH to minimize intramolecular rearrangements. The general strategy used in this study is outlined in Figure 2, and a sample chromatogram illustrating the partial reduction reaction is shown in Figure 3a. In each case, TCEP reduction led to the production of two species in addition to the fully oxidized starting material and the fully reduced end product. These reduction intermediates could be reoxidized with iodine (which results in rapid and irreversible disulfide formation) to regenerate a single form with the HPLC elution time of the starting material, indicating that one of the initial disulfides was retained during the partial reduction and purification.

The purified one-disulfide species were found to undergo very rapid intramolecular rearrangements at the higher pH values (8 to 8.5) required to block the free thiols with alkylating reagents, precluding traditional peptide-mapping methods for identifying the disulfides. Therefore, an alternative technique recently described by Wu and Watson was employed (*20*). In this method, the free thiols are cyanylated at pH 3, and the resulting adducts are induced to undergo an intramolecular reaction that results in cleavage of the peptide bonds preceding the modified Cys residues. HPLC profiles representing a typical cyanylation reaction are shown in Figure 3b. In this reaction, one of the purified one-disulfide forms of 15,25Ala was reacted with a 50-fold molar excess of CDAP for 20 min at 25 °C. Approximately 90% of the peptide was converted to a form with an increased HPLC retention time. Electrospray ionization mass spectroscopy confirmed that this product had the molecular weight expected if the two thiols were cyanylated. Each of the purified one-disulfide forms was reacted with CDAP in the same manner, and in each case the di-cyanylated product was obtained in high yield.

The cyanylated products were purified and then incubated under alkaline conditions, 0.02−1 M NH_4OH, to induce cleavage, as illustrated in Figure 3c for the [1−8] intermediate form of 15,25Ala. The peptide fragments generated by this treatment were purified by HPLC and analyzed by electrospray ionization mass spectrometry. For 11 of the 18 one-disulfide species, the cleavage reactions were sufficiently specific and efficient to positively identify the disulfides when this information was combined with the known identities of the two-disulfide precursors (Figure 2).

Not all cyanylated peptides were cleaved specifically in high yield. As observed previously by Wu and Watson, alkaline treatment of some of the cyanylated peptides resulted

FIGURE 2: Strategy and results for identifying the one-disulfide forms of the four-Cys analogues of ω-MVIIA-Gly. Each of the analogues was fully oxidized to generate the three possible two-disulfide forms, each of which was previously identified by tryptic peptide mapping (*11*). Each was then selectively reduced at low pH, where disulfide rearrangements are minimized, to generate all of the possible one-disulfide intermediates. These forms were subjected to cyanylation and cleavage, as illustrated in Figure 3, to generate peptides with cyanylated N-terminal Cys residues. The peptides indicated were purified and identified by electrospray ionization mass spectrometry. With the exception of the two sequences labeled "K*" at the C- terminus, each of the peptides shown had a mass within two amu of that expected for the sequence shown. These two peptides, which appeared to be generated by cleavage of the peptide bond preceding Cys 25, had masses 14 amu less than expected, which can be accounted for if the peptide bonds were hydrolyzed by attack by the ζ-nitrogen of Lys 24, rather than free ammonia. The disulfide-bonded peptides derived from two forms of 8,20Ala, [15−25] and [1−25] had indistinguishable masses. To ensure that these peptides were correctly identified, their disulfides were reduced, and the larger fragment of each (corresponding to residues 1−15) was subjected to Edman sequencing. The peptide derived from $[1-25]_{8,20Ala}$ yielded the expected sequence, whereas that from $[15-25]_{8,20Ala}$ did not yield phenylthiohydantoin-amino acids, as expected for a peptide with an N-terminal cyanylated Cys residue (*56*). The identities of the one-disulfide forms for which no peptide is shown were inferred from the identities of the other one-disulfide species generated by reduction of the two-disulfide form.

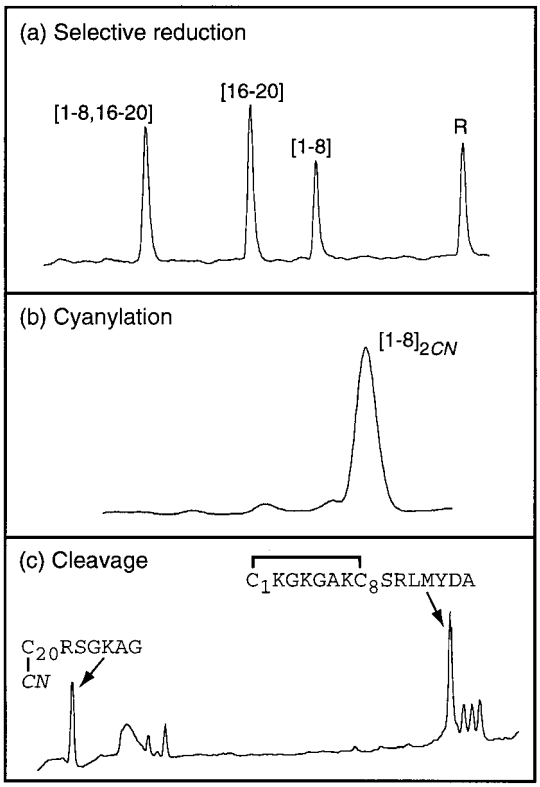

FIGURE 3: Peptide mapping of one-disulfide forms of the 15,25Ala analogue. (a) Selective reduction of $[1-8,16-20]_{15,25Ala}$. The purified two-disulfide form was treated with 10 mM TCEP in 0.1% TFA at 25 °C for 20 min and then fractionated by reversed-phase HPLC as shown. (b) Cyanylation of $[1-8]_{15,25Ala}$. The material from the peak labeled [1−8] in panel a was incubated with a 50-fold molar excess of CDAP for 20 min at pH 3.0 and 25 °C. The resulting material was purified by HPLC as illustrated and was shown by mass spectrometry to be cyanylated at two sites. (c) Cleavage of cyanylated $[1-8]_{15,25Ala}$. The cyanylated peptide was incubated in NH_4OH at 25 °C, and the resulting fragments were purified by reversed-phase HPLC. The fragments were identified by mass spectrometry.

primarily in β-elimination—removal of the γ-sulfur as well as the cyano group from the cyano-cysteine without backbone cleavage (*20*). In addition, several of the reactions yielded small amounts of numerous products, suggesting that nonspecific cleavage occurred when the peptides were incubated with the base. As a consequence, some of the one-disulfide species could not be directly identified. For each of these cases, however, the other one-disulfide product of reducing the two-disulfide species was positively identified, making it possible to infer the identity of the other species. For instance, even though the identity of $[1-16]_{15,25Ala}$ was not confirmed directly, the other product of reducing $[1-16,8-20]_{15,25Ala}$ (with the 8−20 disulfide) was positively identified by peptide mapping.

An unexpected result arose for the species in which Cys 25 was cyanylated. Although cleavage of the peptide bond preceding this residue was observed, the resulting products had masses that were 16 amu smaller than expected. The identities of these peptides, and the corresponding one-disulfide intermediates, were confirmed by further digesting the peptides with trypsin and identifying the resulting fragments, which had the expected masses. The smaller than expected masses of the direct cleavage produces can be accounted for if the ζ-nitrogen of Lys 24, rather than

ammonia, served as a nucleophile to attack the carbonyl carbon of the same residue, resulting in a cyclic structure. This cleavage mode may occur at other Lys−Cys sites, or it may reflect the presence of the Gly residue following the Cys or the proximity of the Cys residue to the peptide C-terminus.

The combined results of the experiments described above thus enabled us to identify all 18 one-disulfide species. The rates and equilibria for forming these species were then determined as described in the following sections.

Rearrangement of One-Disulfide Intermediates. Once a first disulfide forms during oxidative refolding of a protein with more than two Cys residues, this step is typically followed by rapid intramolecular rearrangements that yield other possible one-disulfide intermediates (*27*). Unless there are unusually large kinetic barriers to the formation or rearrangement of specific species, this process leads to a steady-state distribution of intermediates that reflects their relative thermodynamic stabilities.

To confirm that the one-disulfide forms of the various four-Cys analogues readily interconvert with one another, each was isolated at low pH and then allowed to reequilibrate in folding buffer containing no thiol or disulfide reagent. The progress of these reactions was followed by reversed-phase HPLC. During the reactions, there was little or no formation of fully reduced protein or two-disulfide forms, as could occur by either oxidation by molecular oxygen or intermolecular thiol-disulfide exchange. In most cases, the rearrangement process appeared to be complete before the first sample was analyzed 30 s after initiating the reaction, and all but one of the reactions were complete within two minutes. The reaction initiated with $[15-16]_{8,20Ala}$, however, took 5 min to reach an apparent end point. Forming a disulfide between adjacent Cys residues is believed to require either a cis or nonplanar conformation of the intervening peptide bond (*28*), and this conformation may lead to steric hindrance that inhibits exchange with other Cys thiols. For each of the analogues, a very similar end-point distribution was generated regardless of which one-disulfide form was used as the starting material (Figure 4), indicating that these distributions reflect the thermodynamic stabilities of the various species.

The relative steady-state concentrations of the various species are listed in Table 1. In general, the most abundant species were those with the smallest number of residues between the disulfide-bonded Cys residues. A notable exception was $[15-16]_{8,20Ala}$, which accumulated to a lower level than forms with larger loops, almost certainly because of the special steric requirements for forming a disulfide between adjacent residues.

To determine whether noncovalent interactions might preferentially favor some of the one-disulfide forms, the equilibration experiments were repeated in the presence of 8 M urea (Table 1). In general, the denaturant had only small effects on the equilibrium distributions. However, the relative concentrations of the two species containing the 8−20 disulfide (in the 15,25Ala and 1,16Ala analogues) were decreased significantly (by 2.5- or 4-fold) in the denaturant, suggesting that this native disulfide may be stabilized by noncovalent interactions.

Kinetics of Disulfide Formation and Reduction in the Four-Cys Analogues. The equilibration experiments described in the previous section provide a measure of the relative stabilities of the various species formed by each of the analogues, but do not provide a means of comparing the stabilities of disulfide-bonded species formed by the different analogues. To obtain this additional information, we carried out folding experiments with each of the three analogues under conditions where disulfide formation and reduction were promoted by exchange with the oxidized and reduced forms of glutathione (GSSG and GSH, respectively). The equilibrium constants derived from such experiments provide a measure of the peptide disulfide stabilities relative to that of the intermolecular disulfide of glutathione, which then serves as a common reference.

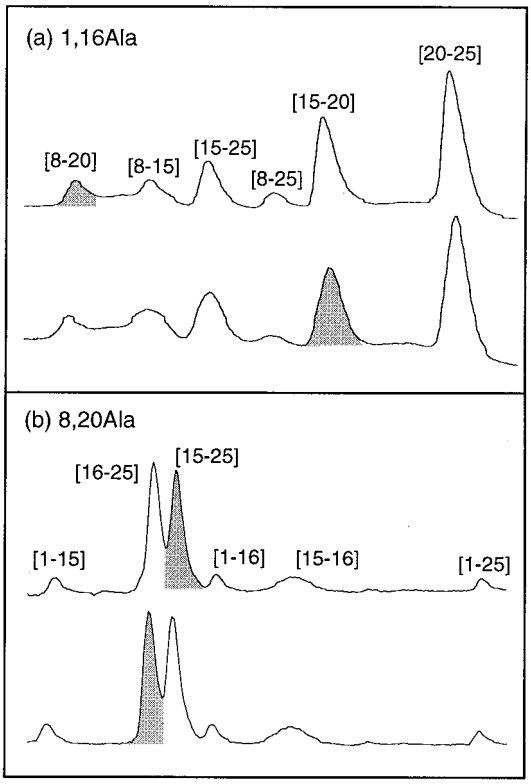

FIGURE 4: Equilibration of one-disulfide forms of (a) 1,16Ala and (b) 8,20Ala analogues of ω-MVIIA-Gly. Purified one-disulfide forms of the indicated analogues were incubated for 1 min in a solution containing 0.1 M Na-MOPS pH 7.3, 0.2 M KCl, and 0.001 M EDTA at 25 °C. The reactions were quenched by acidification, and the intermediates were fractionated by reversed-phase HPLC. The peaks containing the initial intermediate used in each experiment are shaded.

After fully reducing the disulfides, folding was initiating by mixing the peptides with mixtures of GSSG and GSH at pH 7.3, 25 °C. After appropriate time intervals, samples of the folding mixtures were quenched by acidification and analyzed by reversed-phase HPLC. For each of the analogues, at least three folding experiments were carried out, with 0.15 mM GSSG and GSH concentrations of 1, 2, or 5 mM.

Formation of a disulfide by exchange with GSSG is a two-step process: reaction of the reagent with a protein thiol followed by an intramolecular thiol-disulfide exchange reaction to generate the protein disulfide. Because of the relatively low GSSG concentration used, the rate of forming an initial mixed disulfide is expected to be much slower than the subsequent intramolecular step. As a consequence, the

Table 1: Equilibrium Distributions of One-Disulfide Intermediates Bottom

analogue	intermediate[a]	fraction of population[b] 0 M urea	8 M urea
1,16Ala			
	[8−15]	0.05	0.04
	[8−20]	0.04	0.01
	[8−25]	0.02	0.02
	[15−20]	0.25	0.24
	[15−25]	0.13	0.1
	[20−25]	0.51	0.6
8,20Ala			
	[1−15]	0.04	0.05
	[1−16]	0.05	0.03
	[1−25]	0.03	0.02
	[15−16]	0.12	0.22
	[15−25]	0.39	0.33
	[16−25]	0.36	0.35
15,25Ala			
	[1−8]	0.22	0.23
	[1−16]	0.05	0.03
	[1−20]	0.02	0.01
	[8−16]	0.11	0.09
	[8−20]	0.24	0.09
	[16−20]	0.36	0.54

[a] The intermediates with native disulfides are highlighted with bold type. [b] The equilibrium populations of the intermediates were determined by isolating individual intermediates by reversed-phase HPLC, allowing the intermediates to reequilibrate at pH 7.3 and then analyzing the distributions by HPLC, as illustrated in Figure 4.

observed rates of disulfide formation reflect the rate of forming the mixed disulfide, and there is minimum accumulation of the mixed disulfide intermediate (*29*, *30*). The excess of GSH relative to GSSG further ensures that there is minimum accumulation of mixed disulfides at equilibrium. In view of these considerations, the kinetic data were analyzed by comparing the observed time-dependent changes in the concentrations of the various species with those predicted by numerical simulations based on the following model:

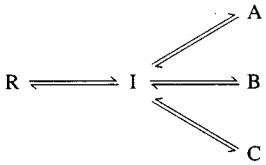

(2)

where R represents the fully reduced protein, I is the total population of one- disulfide intermediates, and A, B, and C are the three possible two-disulfide species. As discussed in the previous section, the one-disulfide intermediates are in rapid equilibrium on the time scale of these experiments (1−60 min), and these species were treated a homogeneous kinetic class. (Although $[15-16]_{8,20Ala}$ undergoes exchange more slowly than the other intermediates, its concentration relative to the other one-disulfide species also remained constant during the experiments.) On the other hand, because the two-disulfide forms contain no free thiols, they cannot interconvert without first being reduced and are treated as individual species. For each analogue, the observed data from all of the experiments could be well fit using this model and a single set of rate constants, as illustrated in Figure 5 for 1,16Ala.

The rate constants derived from these experiments are summarized in Table 2, along with those from parallel

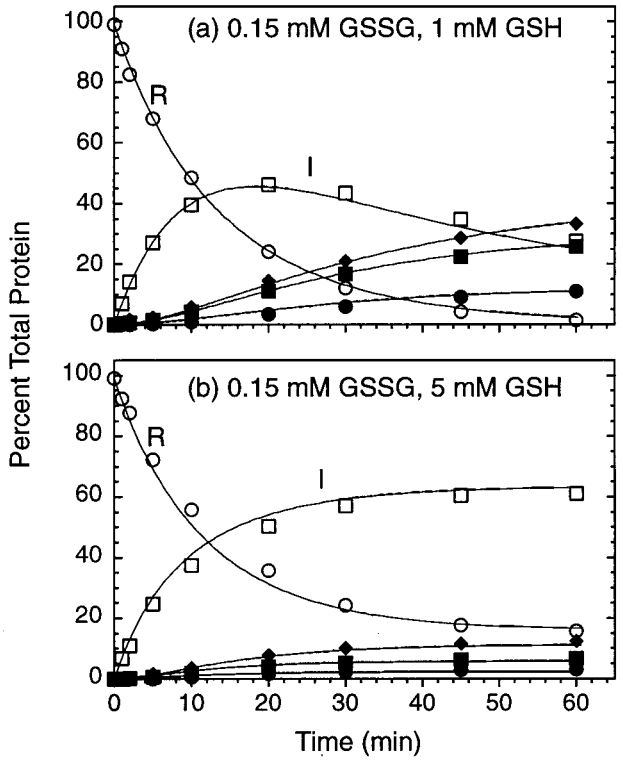

FIGURE 5: Kinetics of disulfide formation in the 1,16Ala analogue of ω-MVIIA-Gly. The fully reduced analogue was purified by HPLC and incubated with the indicated concentrations of GSSG and GSH, 0.1 M Na-MOPS pH 7.3, 0.2 M KCl, and 0.001 M EDTA at 25 °C. At the indicated times, the reactions were quenched by acidification, and the concentrations of the various species were determined by reversed-phase HPLC. The measured concentrations are indicated by the symbols: ○, reduced; □, one-disulfide intermediates; ●, [8−20,15−25]; ♦, [8−25,15−20]; ■, [8−15,20−25]. The curves shown were generated by numerical integration based on the kinetic scheme of eq 2 and the rate constants in Table 2.

Table 2: Rate Constants for Disulfide Formation and Reduction in Four-Cys Analogues of ω-MVIIA-Gly at 25 °C, pH 8.7

analogue	step	formation ($s^{-1}M^{-1}$) 0 M urea	8 M urea	reduction ($s^{-1}M^{-2}$) 0 M urea	8 M urea
1−16Ala					
	R ⇌ I	8.5	3.8	11	7
	I ⇌ [8−15,20−25]	2.1	1.5	120	140
	I ⇌ **[8−20,15−25]**	0.9	0.15	120	50
	I ⇌ [8−25,15−20]	2.4	1.2	70	35
8−20Ala					
	R ⇌ I	9.6	4.9	22	16
	I ⇌ [1−15,16−25]	2.3	1.2	350	410
	I ⇌ **[1−16,15−25]**	2.4	1.2	370	470
	I ⇌ [1−25,15−16]	0.7	0.7	450	720
15,25Ala					
	R ⇌ I	13	6.9	30	21
	I ⇌ [1−8,16−20]	5	4.3	12	100
	I⇌ **[1−16,8−20]**	0.5	0.1	120	30
	I ⇌ [1−20,8−16]	0.9	0.25	140	50

experiments carried out in the presence of 8 M urea. The second-order rate constants for forming the initial disulfides lay in the range of 8.5 to 13 s^{-1} M^{-1}. Since each reduced analogue contains four Cys residues, these rates are consistent with previous results indicating that the rate constant for exchange between a single thiol in a positively charge peptide and GSSG under these conditions is typically about 0.5−2 s^{-1} M^{-1} (*31*, *32*).

The rate constants for forming the second disulfides were generally lower than those for the first disulfide, as expected since the precursors contain only two Cys thiols. These rate constants also varied quite widely for the different two-disulfide products, from 0.5 to 5 s^{-1} M^{-1}. This variation is also expected, since the precursors for the various two-disulfide forms were present at different concentrations in the population of one-disulfide precursors.

A wide range was also observed for the third-order rate constants for reducing the various species with one and two disulfides, from 11 to 450 s^{-1} M^{-2}, with the rates for reducing the two-disulfide forms uniformly greater than those for the first disulfide. Although these differences might be taken to mean that the two-disulfide forms are less stable than their one-disulfide precursors, the differences in reduction rate can largely be accounted for by statistical factors that distinguish the two types of reaction, as discussed in the appendix.

The kinetics of disulfide formation and reduction were also measured for the three analogues in the presence of 8 M urea. As indicated in Table 2, the strong denaturant generally had only small effects on the observed rates, suggesting that there is relatively little stable structure in most of the one- or two-disulfide species.

Because the individual rate constants for disulfide formation and reduction by exchange with GSSG and GSH are strongly influenced by the thiol-disulfide exchange chemistry and statistical factors, they provide relatively little direct information about the conformational properties of the polypeptides. The rate constants can, however, be used to calculate equilibrium constants for the various disulfide formation steps, and these allow a quantitative comparison of the conformational tendencies to form the different disulfides at different stages of folding, as discussed in the following sections.

Effective Concentrations of Cys Thiol Pairs in the Fully Reduced Peptides. The overall reaction for forming a single-disulfide bond via exchange with GSSG can be summarized as:

$$P_{SH}^{SH} + GSSG \rightleftharpoons P_S^S + 2GSH \quad (3)$$

where P_{SH}^{SH} and P_S^S represent the dithiol and disulfide forms of the protein, respectively. The equilibrium constant is given by:

$$K_{SS} = \frac{[P_S^S][GSH]^2}{[P_{SH}^{SH}][GSSG]} \quad (4)$$

This equilibrium constant reflects the stability of the intramolecular protein disulfide relative to that of a chemically equivalent intermolecular disulfide. The constant has units of concentration and can be thought of as an "effective concentration", C_{eff} (*33*−*35*). In unfolded polypeptides, effective concentrations typically lie in the range of 0.001 to 0.1 M (*36*−*38*), while those in native proteins can be as large as 10^5 M (*29*).

The overall equilibrium constants for forming the one-disulfide intermediates can be calculated from the rate constants for forming and reducing this population. To calculate the effective concentration of a particular pair of Cys thiols, however, the overall equilibrium constant must be multiplied by a fraction representing the concentration of the specific one-disulfide species in the total population, as listed in Table 1. The effective concentrations calculated in this way are designated C_{eff}^1 to indicate that they represent formation of a first disulfide and are summarized in Table 3. The calculated values ranged from 0.01 to 0.5 M.

Table 3: Effective Concentrations of Cys Thiol Pairs in Reduced ω-MVIIA-Gly Analogues

		C_{eff}^1 (M)[b]	
analogue	Cys pair[a]	0 M urea	8 M urea
1,16Ala			
	8−15	0.039	0.022
	8−20	0.031	0.005
	8−25	0.015	0.011
	15−20	0.19	0.13
	15−25	0.10	0.054
	20−25	0.39	0.33
8,20Ala			
	1−15	0.017	0.015
	1−16	0.022	0.009
	1−25	0.013	0.006
	15−16	0.052	0.067
	15−25	0.17	0.10
	16−25	0.16	0.11
15,25Ala			
	1−8	0.095	0.076
	1−16	0.022	0.010
	1−20	0.009	0.003
	8−16	0.048	0.030
	8−20	0.10	0.030
	16−20	0.16	0.18

[a] The disulfides of the native protein are indicated by bold type. [b] Effective concentrations represent the equilibrium constants for forming a disulfide between the indicated Cys thiol pairs in the fully reduced protein via exchange with GSSG. Calculated from the rate constants of Table 2 and the distribution of one-disulfide intermediates (Table 1) as described in the text.

Each of the native disulfides (1−16, 8−20, and 15−25) can be formed by two of the three analogues, thus providing a check for consistency in the results obtained with the three independent sets of experiments. For the 1−16 and 15−25 disulfides, the independent measurements gave results that differed by 2-fold or less, both with and without urea. On the other hand, C_{eff}^1 measured for 8−20 was significantly greater in the 1,16Ala analogue than in 15,25Ala, by factors of 3.4 and 5.7 in 0 and 8 M urea, respectively. It is possible that the Ala replacements in one or both of these analogues may have perturbed the conformation and energetics of the reduced peptide or the [8−20] intermediate. However, the small magnitude of these energetic effects, on the order of 1 kcal/mol, may make it quite difficult to determine their origin, even with the aid of high-resolution structure analysis.

In Figure 6 the effective concentrations (except for the vicinal disulfide between Cys 15 and Cys 16) are plotted as a function of the loop length (N) for the individual disulfides, demonstrating the expected inverse relationship. The data were fit to a function of the form:

$$C_{eff} = aN^b \quad (5)$$

as predicted for a random-walk polymer, where a and b are empirical constants. For the measurements made in the absence of urea, the estimated exponent, b, was -1.3 ± 0.4, and was -1.7 ± 0.5 in the presence of 8 M urea. These values are consistent with that predicted by simple random-

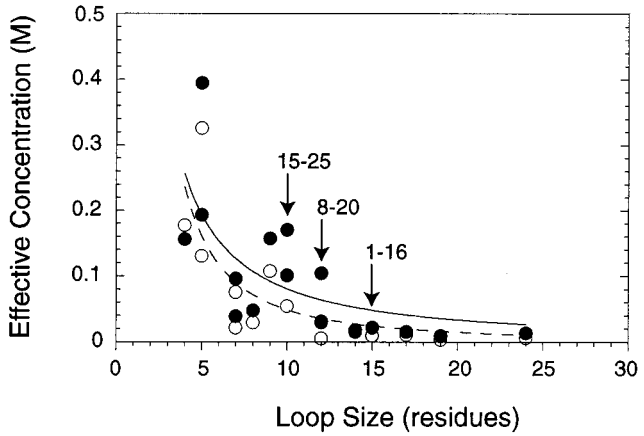

FIGURE 6: Effective concentrations, C^1_{eff}, of Cys thiol pairs in reduced four-Cys analogues in 0 M (filled symbols) and 8 M urea (open symbols). The effective concentrations were calculated from the relative populations of the one-disulfide intermediates in Table 1 and the rate constants of Table 2, as described in the text, and are plotted as a function of the number of residues between the Cys residues. The solid and dashed lines represent nonlinear least-squares fits of the data for 0 and 8 M urea, respectively, to the power function: $C_{eff} = aN^b$. For 0 M urea, $a = 1.5 \pm 1$ M and $b = -1.3 \pm 0.4$, and for 8 M urea, $a = 2.6 \pm 2$ M and $b = -1.7 \pm 0.4$. The arrows indicate the effective concentrations for the native disulfides, each of which is represented in two of the analogues.

walk models of disordered chains ($b = -1.5$) (*39*), but are somewhat lower than those predicted from lattice simulations that include the effects of excluded volume, which predict $-2 \geq b \geq -2.4$ (*40*). Although the difference may not be significant, the more negative exponent observed in the presence of 8 M urea may reflect more favorable solvation of the chain under these conditions, which would tend to increase the average dimensions of the chain and decrease the probability of long-range interactions.

For the Cys 15−Cys 16 disulfide, the effective concentrations were 0.052 and 0.067 M in 0 and 8 M urea, respectively, significantly smaller than that seen for the loops formed with four or five intervening residues. These values are similar to that measured by Zhang and Snyder (*36*) for a vicinal disulfide in a short peptide (about 100 mM) and clearly demonstrate that formation of such a disulfide can be quite significant even in the absence of any specific structure to stabilize it.

In principle, the effective concentrations calculated from equilibrium constants may reflect the presence of any stable structure in the one-disulfide intermediates, and it has been suggested that more reliable and direct information about the conformational properties of a reduced protein may be obtained from effective concentrations determined from the ratio of intramolecular and intermolecular rate constants (*37*, *38*). In the case of the ω-MVIIA-Gly analogues, however, the small effects of urea on the equilibrium effective concentrations suggest that there is relatively little stable structure in either the reduced protein or the one-disulfide intermediates. The most pronounced exception may be the [8−20] intermediate, which contains a native disulfide and can be formed by either the 1,16Ala or 15,25Ala analogues. In these analogues, the addition of 8 M urea decreased C^1_{eff} for the 8−20 disulfide by 5.5- and 3.3-fold, respectively. These changes reflect primarily a decrease in the concentration of [8−20] in the one-disulfide populations and may be due to some marginally stable structure in this intermediate, although neither of the values determined for C^1_{eff} in the absence of urea appears to be exceptionally large for the loop length. Overall, the correlation with loop size and the small effects of urea suggest that the effective concentrations primarily reflect the probabilities of forming the various disulfides in the reduced and largely disordered polypeptides.

Table 4: Effective Concentrations of Cys Thiol Pairs in One-Disulfide Intermediates

			C^2_{eff} (M)[b]	
analogue	Cys pair[a]	preexisting disulfide[a]	0 M urea	8 M Uurea
1,16Ala				
	8−15	20−25	0.034	0.018
	8−20	**15−25**	0.058	0.03
	8−25	15−20	0.14	0.14
	15−20	8−25	1.7	1.7
	15−25	**8−20**	0.19	0.3
	20−25	8−15	0.35	0.27
8,20Ala				
	1−15	16−25	0.018	0.0084
	1−16	**15−25**	0.017	0.0077
	1−25	15−16	0.013	0.0044
	15−16	1−25	0.052	0.049
	15−25	**1−16**	0.13	0.08
	16−25	1−15	0.16	0.058
15,25Ala				
	1−8	16−20	0.12	0.08
	1−16	**8−20**	0.017	0.037
	1−20	8−16	0.058	0.056
	8−16	1−20	0.32	0.50
	8−20	**1−16**	0.083	0.11
	16−20	1−8	0.19	0.19

[a] The disulfides of the native protein are indicated by bold type. [b] Effective concentrations represent the equilibrium constants for forming a disulfide between the indicated Cys thiol pairs in the precursor one-disulfide intermediate via exchange with GSSG. Calculated from the rate constants of Table 2 and the distribution of one- disulfide intermediates (Table 1) as described in the text.

Effective Concentrations for Forming a Second Disulfide in the One-Disulfide Intermediates. The measured rate constants can also be used to compare the relative tendency to form a given disulfide in the fully reduced protein with that for forming the same disulfide in an intermediate with a preexisting disulfide. For a polypeptide with six Cys residues, each of the 15 one-disulfide intermediates can form six possible second disulfides, leading to a total of 90 different possible reactions (but only 45 products, since each may be formed via two pathways). With the set of four-Cys analogues used in these studies the number of combinations is reduced to only 18, since each one-disulfide species can form only a single second disulfide. These combinations include each of the three native disulfides in combination with each of the other two native linkages, as well as each of the 12 non-native disulfides in the presence of one other non-native bond.

The equilibrium constants calculated from the rate constants for forming and reducing the two-disulfide species represent the reactions from the entire one-disulfide population. To calculate the effective concentrations corresponding to the formation of a disulfide from a specific one-disulfide precursor, designated C^2_{eff}, the overall equilibrium constant was divided by the fraction representing the concentration of the precursor in the one-disulfide population. The resulting effective concentrations are listed in Table 4, measured in both 0 and 8 M urea. In general, the values of C^2_{eff} display

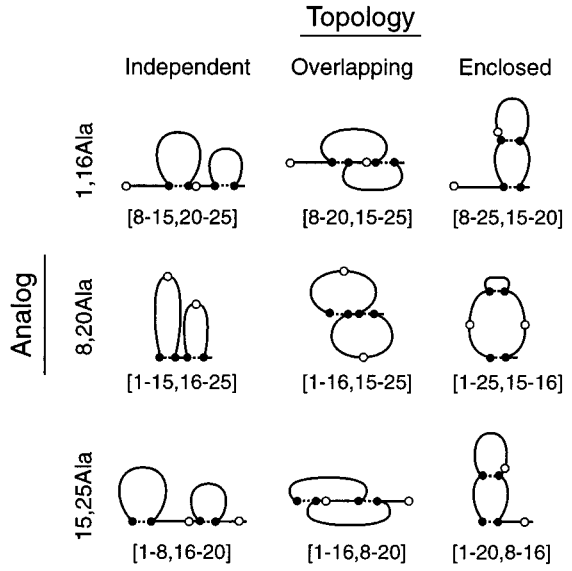

FIGURE 7: Schematic representations of the topological patterns in the two-disulfide forms of ω-MVIIA-Gly. The disulfide bonds in the intermediates are indicated by dashed lines between the filled circles representing the Cys residues, and the nondisulfide bonded Cys residues (replaced with Ala in the analogues) are indicated by open circles. The native intermediates are shown in the center column, and all possess the overlapping topology.

Table 5: Influence of Pre-existing Disulfides on Effective Concentrations

analogue	2-disulfide intermediate[a]	topology[b]	C^2_{eff}/C^1_{eff}[c] −urea	C^2_{eff}/C^1_{eff}[c] +urea	C^3_{eff}/C^2_{eff}[d] −urea	C^3_{eff}/C^2_{eff}[d] +urea
1,16Ala						
	[8−15,20−25]	independent	0.9	0.8		
	[**8−20,15−25**]	overlapping	2	6	3000	270
	[8−25,15−20]	enclosed	9	13		
8,20Ala						
	[1−15,16−25]	independent	1	0.5		
	[**1−16,15−25**]	overlapping	0.8	0.8	1800	180
	[1−25,15−16]	enclosed	1.0	0.7		
15,25Ala						
	[1−8,16−20]	independent	1	1		
	[**1−16,8−20**]	overlapping	0.8	4	1000	50
	[1−20,8−16]	enclosed	7	17		

[a] The intermediates with native disulfides are indicated with bold type. [b] The topologies of the two-disulfide intermediates are as illustrated in Figure 7. [c] Calculated from the values in Tables 3 and 4. [d] Calculated from the values in Tables 4 and 6, using the average of the two values for C^2_{eff}.

a range similar to that seen for C^1_{eff}, although some are notably larger, in one case (for forming the 15−20 disulfide in the presence of 8−25) exceeding 1 M.

As illustrated schematically in Figure 7, forming two disulfides in any of the four-Cys analogues can generate three distinct topologies: (a) two independent loops, (b) two overlapping loops, and (c) one loop fully enclosed by the other. As a measure of the extent to which the two disulfides favor one another, the ratios C^2_{eff}/C^1_{eff} for each disulfide pair are listed in Table 5. By thermodynamic linkage, this ratio is expected to be the same for the two disulfides in a given two-disulfide species, an assumption that is implicit in the methods used here to calculate the effective concentrations.

For the three species with independent loops, there was very little effect of one disulfide on the formation of the other. At the other extreme, two of the species with fully enclosed loops ($[8-25,15-20]_{1,16Ala}$ and $[1-20,8-16])_{15,25Ala}$) displayed C^2_{eff}/C^1_{eff} ratios of approximately 8 in the absence of urea and 15 in 8 M urea. These increases are qualitatively consistent with the predictions of models based on an idealized random-flight chain, in which the inner loop can be thought to shorten the loop formed by the outer two Cys residues, as well as by simulations based on three-dimensional lattice models, which also include excluded-volume effects (*40*). The larger effects seen in the presence of urea may reflect a greater expansion of the polypeptide under conditions of better solvation, although the observed differences of about 2-fold may not be significant. In the third species with an enclosed loop, $[1-25,15-16]_{8,20Ala}$, the two disulfides did not significantly influence one another. This result is perhaps not surprising, since the disulfide between adjacent residues should affect only the local geometry of the polypeptide.

For the three disulfide pairs that result in overlapping loops, the ratios C^2_{eff}/C^1_{eff} were only slightly different from 1 in the absence of urea, but the ratio was considerably larger in the presence of 8 M urea for two of the pairs, $[8-20,-15-25]_{1,16Ala}$ and $[1-16,8-20]_{15,25Ala}$. Lattice model simulations predict a range of effects between disulfides with topologies of this type, depending on the exact positions of the linkages (*40*). When the central linked residues are close together, the two bonds are predicted to inhibit one another, as observed for $[1-16,15-25]_{8,20Ala}$. The molecules with the overlapping topology are, in fact, the ones containing the native disulfide pairs, and the relatively small values of C^2_{eff}/C^1_{eff} indicate that there is very little cooperativity among the native disulfides at this stage of folding.

Effective Concentrations for Forming a Third Disulfide. The data obtained for the four-Cys analogues were also used to estimate the effective concentrations for forming the third native disulfide, C^3_{eff}, in the three forms of the unmodified protein with two native disulfides (*11*). The overall reaction for forming the three disulfides can be divided into two components, formation of a precursor with two native disulfides (II_N) and formation of the third disulfide:

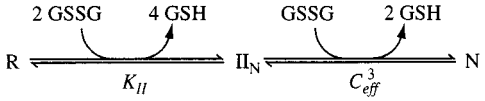

(6)

where K_{II} is the overall equilibrium constant for forming II_N from R. There are, in principle, three pathways of this form, although they may not all play a significant kinetic role in the folding of the unmodified protein. Provided that the Cys → Ala replacements have minimal effects on the stabilities and conformational properties of the two-disulfide forms, the three values of K_{II} can be estimated from the rate constants measured in this study for the four-Cys analogues. The values of C^3_{eff} for forming the three native disulfides can then be estimated as:

$$C^3_{eff} = \frac{K_{III}}{K_{II}} \quad (7)$$

where K_{III} is the overall equilibrium constant for forming the native protein with three disulfides from the fully reduced polypeptide. By measuring the equilibrium concentrations of the native and fully reduced forms of ω-MVIIA-Gly in

Table 6: Effective Concentrations of Cys Thiol Pairs in Intermediates with Two Native Disulfides

		0 M urea		8 M urea	
Cys pair	intermediate	K_{II} (M^2)[a]	C^3_{eff} (M)[b]	K_{II} (M^2)[a]	C^3_{eff} (M)[b]
1−16	[8−20,15−25]	5.8×10^{-3}	50	1.6×10^{-3}	6
8−20	[1−16,15−25]	2.8×10^{-3}	110	7.8×10^{-4}	12
15−25	[1−16,8−20]	1.8×10^{-3}	170	1.1×10^{-3}	9

[a] Overall equilibrium constant for forming the two native disulfides in the fully reduced analogue missing the indicated Cys pair. Calculated from the rate constants of Table 2. [b] The effective concentration of the two thiols in the intermediates with two native disulfides were calculated by dividing K_{III} (the overall equilibrium constant for forming all three disulfides in the unmodified protein) by the value of K_{II} for the analogue lacking the Cys pair (eq 7 in the text)

the presence of GSSG and GSH, K_{III} was estimated to be 0.3 ± 0.04 and 0.01 ± 0.001 M^3 in 0 and 8 M urea, respectively. Values of C^3_{eff} for the three native disulfides under the two sets of conditions were calculated using these values and the rate constants in Table 2.

The resulting effective concentrations (Table 6) and the ratios C^3_{eff}/C^4_{eff} (Table 5) indicate that the presence of any two of the three native disulfides greatly enhances formation of the third. In the absence of urea, the values of C^3_{eff} ranged from 50 to 170 M, about 1000-fold larger than those observed when these disulfides were formed in the fully reduced protein or in intermediates with one other native disulfide. Addition of 8 M urea decreased C^3_{eff} by about 10-fold, but the resulting values were still about 100-fold greater than those for the earlier disulfide-formation steps.

These results indicate that each of the intermediates with two native disulfides is probably stabilized by noncovalent interactions that favor forming the third disulfide. It also appears, however, that the topological constraints imposed by the first two native disulfides may be sufficient to significantly favor the third, as discussed further below.

Implications for Folding Mechanisms of ω-Conotoxins. The effective concentrations determined here for forming the native disulfides of ω-MVIIA-Gly are summarized in Figure 8 in the form of a schematic pathway. It should emphasized, however, that this scheme represents only the relative equilibria for forming the native disulfides and is not meant to indicate a kinetic mechanism, which would also include non-native species and intramolecular rearrangements. The scheme illustrates that the native disulfides form in a cooperative fashion: The effective concentrations of the Cys thiol pairs increase from about 0.1 M in the fully reduced peptide (Table 3) to about 100 M in the intermediates with two native disulfides (Table 5). Non-covalent interactions also act to enhance the stabilities of the disulfides, as demonstrated by the effects of 8 M urea on the formation of the final disulfide. Together, the disulfides and noncovalent interactions are sufficient to significantly favor the native configuration, so that the fully reduced peptide refolds with an efficiency of about 90% under conditions where the native form can freely interconvert with forms with non-native disulfides. Other members of the ω-conotoxin have also been found to refold with modest efficiency, as have some other proteins with the same overall fold and pattern of disulfide bonds (*15*, *41*, *42*). The ability of these molecules to fold spontaneously to a well-defined conformation was initially somewhat surprising given their small size and high degree

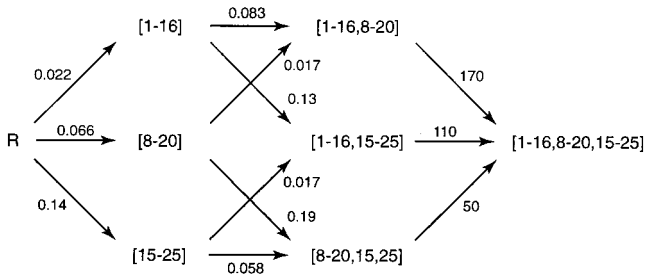

FIGURE 8: Effective concentrations for forming the native disulfides during the refolding of reduced ω-MVIIA-Gly, as deduced by analysis of the three four-Cys analogues. The effective concentrations have units of molarity and represent the equilibrium constants for forming the disulfides by exchange with glutathione. Note that all of the upward pointing arrows represent the formation of the 1−16 disulfide in different contexts; the horizontal arrows represent formation of the 8−20 disulfide; and the downward pointing arrows represent formation of the 15−25 disulfide. The effective concentrations for forming the one-disulfide intermediates are the means of the values determined for the two analogues containing the two relevant Cys residues. Because the values determined for the same disulfide in different analogues are not identical, the values shown in this figure do not satisfy exactly the principle of microscopic reversibility.

of sequence variation, and this ability may make the ICK fold particularly attractive as a scaffold for the design of new peptides with novel binding activities (*10*).

Given the small size of the ω-conotoxins and the particularly important role the disulfides play in their stabilities, it might be expected that the evolved topology of disulfide bonds would be one that is optimized to form efficiently. It appears, however, that nearly the opposite is true. The loops formed by the native disulfides are relatively long, with spacings of 10, 12, and 15 residues, and the effective concentrations of these Cys thiol pairs in the fully reduced protein are lower than for pairs that form shorter loops (Table 3 and Figure 6). In addition, the loop defined by each native disulfide forms an overlapping topology with each of the others (Figure 7), an arrangement that leads to little or no enhancement of the effective concentrations for forming a second native disulfide. Thus, initial formation of the native disulfides does not appear to be particularly favored by either the loop sizes or their topologies. On the other hand, once the disulfides are present, those that are least favored in the unfolded state are expected to make the largest contributions to the stability of the native protein, since these linkages have the largest effect on the entropy of the unfolded chain (*43*, *44*). Perhaps the "cysteine-knot" topology seen in the ω-conotoxins and other small proteins has been selected in evolution because this arrangement leads to relatively large stabilizing contributions from the disulfides.

Once two native disulfides are formed, there is a very large increase in the effective concentration of the remaining two thiols. Even in the presence of 8 M urea, the values calculated for C^3_{eff} are 50−250-fold greater than those for forming the same disulfides when only one other native disulfide is present. These large effects are not readily explained in terms of the covalent topologies of the intermediates. For instance, once the 8−20 disulfide is present, adding the 15−25 disulfide does not, in a covalent sense, bring Cys 1 and 16 closer together (Figure 7). The large effective concentrations are also surprising in view of available data concerning the conformational properties of the two-disulfide forms. Circular

dichroism spectroscopy indicates that these molecules lack most of the native secondary structure, and their affinity for Ca^{2+} channels is 100- to 10 000-fold lower than that of native ω-MVIIA-Gly (*11*). They are presumably even less structured in the presence of 8 M urea. It is possible, however, that these intermediates contain some partial structure that brings the remaining two Cys thiols together and is especially resistant to chaotropic denaturants.

In addition to forming cooperatively, the native disulfides are significantly favored relative to non-native ones (*16*). Unfortunately, the data available are not sufficient to calculate effective concentrations of non-native disulfides in species with two disulfides, since the appropriate three-disulfide forms have not been identified. Thus, it is not known whether the presence of any two disulfides significantly favors a third or, alternatively, the native topology is especially favorable. It is clear, however, that the presence of 8 M urea significantly destabilizes the native structure relative to those with non-native disulfides, suggesting that some of the specificity arises from the hydrophobic effect. As noted previously, the hydrophobic core of the ω-conotoxin fold is composed almost entirely of the disulfide-bonded Cys residues, and the native structure may be favored because this arrangement of disulfides is most effective in burying the non- polar surface area (*15*).

Overall, our results indicate that the folding of ω-MVIIA-Gly takes place in two distinct phases. Initially, the first and second disulfides form with little or no specificity, and the presence of the first native disulfide does not significantly favor a second. Once two native disulfides are formed, however, the third is strongly favored, and this preference depends, in part, on the hydrophobic effect. Further progress in understanding the remarkable ability of these small molecules to fold efficiently will likely require structural characterization of the intermediates with two native disulfides, for it is in these intermediates and the native structure that the cooperativity of folding is expressed.

Possible Implications for the Role of Topology in Protein Folding. Over the past few years, there has been growing interest in the role of chain topology in determining folding mechanisms and rates (*45*−*48*), an interest that has been greatly stimulated by the striking observation of Plaxco et al. that the folding rates for small proteins with simple kinetics are inversely correlated with relative contact order, a parameter that reflects the average sequence distance between residues that interact in the native protein (*49*). Although the underlying basis for this correlation is not yet clear, it has been suggested that it may reflect the importance of short range interactions in initially reducing the conformational entropy of the unfolded chain and thereby favoring additional interactions between more distantly separated residues (*49*−*51*).

The results summarized in Table 5 confirm theoretical predictions (*40*) that the presence of one interaction can increase the tendency of a second to form. With only one disulfide present, the effects were significant only when the loop formed by one disulfide was fully enclosed by the loop formed by the other, and, in this case, non-native rather than native interactions are favored by this effect. The presence of two native disulfides, however, caused much more dramatic effects, even in the presence of 8 M urea. These observations suggest that a relatively small number of key interactions may be sufficient to direct formation of the native fold, consistent with mutational analyses of folding transition states (*51*, *52*) and a recent computational study (*53*).

ACKNOWLEDGMENT

We thank Drs. W. R. Gray and B. M. Olivera for helpful discussions and Dr. R. Schackmann for synthesizing the peptides used in this study.

APPENDIX

As indicated in Table 2, the rate constants for reduction of the various one- and two-disulfide forms of ω-MVIIA-Gly differed greatly, the rates for reducing the two-disulfide species being about 10-fold greater than for the forms with one disulfide. Although rates of reduction can be greatly influenced by the structural context of a disulfide in a folded or partially folded protein, the differences observed here can largely be accounted for by statistical factors that influence a steady-state equilibrium between the form with the protein disulfide and a mixed-disulfide intermediate (*29*, *30*).

Disulfide reduction by GSH is a two-step process with a mixed-disulfide intermediate, as illustrated below for the simple case of a single disulfide in a polypeptide with only two Cys thiols:

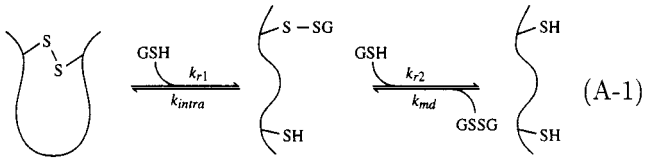

(A-1)

where k_{r1} and k_{r2} are the second-order rate constants for the first and second reduction steps, respectively, k_{intra} is the first-order rate constant for reforming the protein disulfide from the mixed disulfide, and k_{md} is the rate constant for forming a mixed disulfide by reaction of either protein thiol with GSSG. There are two possible mixed-disulfide species, and all of the rate constants shown are assumed to refer to the total rates of forming or converting both in the indicated reactions. (In this and the following schemes, the thiols are shown in the protonated form that predominates at neutral pH, although it is the ionized form, a thiolate, that is actually reactive. The apparent rate constants will be influenced by the thiol pK_a's and the solution pH, as well as by the intrinsic reactivities of the thiolates and disulfides.) Because the reverse of the initial reduction is an intramolecular reaction, it is usually quite fast, and a steady-state equilibrium is established between the protein disulfide form (D) and the mixed disulfide (MD). The steady-state concentration of the mixed disulfide is given by:

$$[\mathrm{MD}] = [\mathrm{D}][\mathrm{GSH}]\frac{k_{\mathrm{r1}}}{k_{\mathrm{intra}}} \qquad \text{(A-2)}$$

The observed rate of reducing the disulfide is determined by the product of the steady-state concentration of the

intermediate, the concentration of GSH, and the rate constant for the second reduction step:

$$\frac{d[\mathrm{D}]}{dt} = -[\mathrm{MD}][\mathrm{GSH}]k_{r2} \quad \text{(A-3)}$$

$$= -[\mathrm{D}][\mathrm{GSH}]^2\frac{k_{r1}k_{r2}}{k_{intra}} \quad \text{(A-4)}$$

The apparent third-order rate constant for reducing the disulfide is then given by:

$$k_{app} = \frac{k_{r1}k_{r2}}{k_{intra}} \quad \text{(A-5)}$$

During the reduction of a single disulfide in a polypeptide with four Cys thiols, the mixed-disulfide species generated directly by reduction of the protein disulfide can also interconvert with two other mixed disulfides. Each of the four mixed-disulfide species can be reduced further or can reform a one-disulfide species. Since the one-disulfide intermediates are treated as a single population in the kinetic scheme (eq 2) used here to analyze the folding of the ω-MVIIA-Gly analogues, the observed third-order rate constants derived from this analysis reflect the steady state-equilibria between all of the one-disulfide intermediates and all of the mixed disulfide species.

The situation is somewhat different, however, for the reduction of a two-disulfide form, as shown in the following scheme:

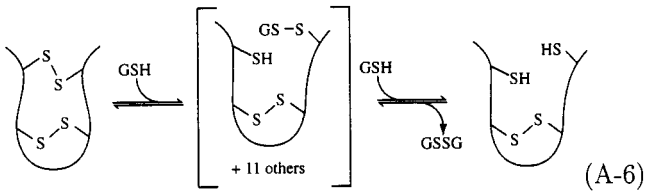

(A-6)

In this case, there are 12 mixed disulfides species that rapidly equilibrate once one disulfide has been broken: Each of the six single-disulfide intermediates can form a mixed disulfide at either of the two free thiols. Only four of these mixed-disulfide intermediates, however, are competent to reform any one of the original two-disulfide species, each of which is treated separately in the analysis (eq 2). In addition, if both disulfides are accessible to the thiol reagent, the rate of the initial exchange reaction with GSH will be approximately twice that for the reaction of a one-disulfide intermediate. Since the steady-state equilibrium depends on the relative rates of reducing and reforming the protein disulfide, these statistical factors predict that the apparent rate constant for reducing a single two-disulfide species will, on average, be approximately 6-fold greater than that for reducing the population of one-disulfide species. Consistent with this prediction, the average rate constant for reducing the two-disulfide species, 206 s^{-1} M^{-2}, was 10-fold greater than that for reducing the one-disulfide populations, 21 s^{-1} M^{-2}. It should be noted, however, that the individual observed rate constants are also expected to depend on the individual rates of the intramolecular disulfide-formation steps (k_{intra}), and the rate for reducing a specific two-disulfide species will be further influenced by the relative concentrations of the various mixed-disulfides intermediates. It is thus quite difficult to interpret the individual rate constants for reduction in terms of the individual species in the populations. As discussed in the text, more detailed information about the individual one- and two-disulfide forms was deduced from the equilibrium constants for disulfide formation and reduction, together with the measured concentrations of the individual intermediates making up the one-disulfide population.

REFERENCES

1. Olivera, B. M., Miljanich, G. P., Ramachandran, J., and Adams, M. E. (1994) *Annu. Rev. Biochem. 63*, 823−867.
2. Miljanich, G. P., and Ramachandran, J. (1995) *Annu. Rev. Pharmacol. Toxicol. 35*, 707−734.
3. Bowersox, S. S., and Luther, R. (1998) *Toxicon 36*, 1651−1658.
4. Davis, J. H., Bradley, E. K., Miljanich, G. P., Nadasdi, L., Ramachandran, J., and Basus, V. J. (1993) *Biochemistry 32*, 7396−7405.
5. Farr-Jones, S., Miljanich, G. P., Nadasdi, L., Ramachandran, J., and Basus, V. J. (1995) *J. Mol. Biol. 248*, 106−124.
6. Nielsen, K. J., Thomas, L., Lewis, R. J., Alewood, P. F., and Craik, D. J. (1996) *J. Mol. Biol. 263*, 297−310.
7. Atkinson, R. A., Kieffer, B., Dejaegere, A., Sirockin, F., and Lefèvre, J. F. (2000) *Biochemistry 39*, 3908−3919.
8. Le-Nguyen, D., Heitz, A., Chiche, L., Castro, B., Boigegrain, R. A., Favel, A., and Coletti-Previero, M. A. (1990) *Biochimie 72*, 431−435.
9. Pallaghy, P. K., Nielsen, K. J., Craik, D. J., and Norton, R. S. (1994) *Protein Sci. 3*, 1833−1839.
10. Craik, D. J., Daly, N. L., and Waine, C. (2001) *Toxicon 39*, 43−60.
11. Price-Carter, M., Hull, M. S., and Goldenberg, D. P. (1998) *Biochemistry 37*, 9851−9861.
12. Flinn, J. P., Pallaghy, P. K., Lew, M. J., Murphy, R., Angus, J. A., and Norton, R. S. (1999) *Biochim. Biophys. Acta 1434*, 177−190.
13. Olivera, B. M., Rivier, J., Clark, C., Ramilo, C. A., Corpuz, G. P., Abogadie, F. C., Mena, E. E., Woodward, S. R., Hillyard, D. R., and Cruz, L. J. (1990) *Science 249*, 257−263.
14. Olivera, B. M., Rivier, J., Scott, J. K., Hillyard, D. R., and Cruz, L. J. (1991) *J. Biol. Chem. 266*, 22067−22070.
15. Price-Carter, M., Gray, W. R., and Goldenberg, D. P. (1996) *Biochemistry 35*, 15537−15546.
16. Price-Carter, M., Gray, W. R., and Goldenberg, D. P. (1996) *Biochemistry 35*, 15547−15557.
17. Goldenberg, D. P., Koehn, R. E., Gilbert, D. E., and Wagner, G. (2001) *Protein Sci. 10*, 538−550.
18. Oyarce, A. M., and Eipper, B. A. (1995) *J. Cell Science 108*, 287−297.
19. Gray, W. R. (1993) *Protein Sci. 2*, 1732−1748.
20. Wu, J., and Watson, J. T. (1997) *Protein Sci. 6*, 391−398.
21. Creighton, T. E. (1978) *Prog. Biophys. Mol. Biol. 22*, 231−298.
22. Goldenberg, D. P. (1992) *Trends Biochem. Sci. 17*, 257−261.
23. Weissman, J. S., and Kim, P. S. (1991) *Science 253*, 1386−1393.
24. Xu, X., Rothwarf, D. M., and Scheraga, H. A. (1996) *Biochemistry 35*, 6406−6417.
25. Chatrenet, B., and Chang, J.-Y. (1992) *J. Biol. Chem. 267*, 3038−3043.
26. Chang, J.-Y. (1996) *Biochemistry 36*, 11702−11709.
27. Creighton, T. E. (1992) *BioEssays 14*, 195−199.
28. Wang, X.-H., Connor, M., Smith, R. A., Maciejewski, M. W., Howden, M. E. H., Nicholson, G. M., Christie, M. J., and King, G. F. (2000) *Nat. Struct. Biol. 7*, 505−513.
29. Creighton, T. E., and Goldenberg, D. P. (1984) *J. Mol. Biol. 179*, 497−526.
30. Creighton, T. E. (1986) *Methods Enzymol. 131*, 83−106.

31. Szajewski, R. P., and Whitesides, G. M. (1980) *J. Am. Chem. Soc. 102*, 2011−2026.
32. Bulaj, G., Kortemme, T., and Goldenberg, D. P. (1998) *Biochemistry 37*, 8965−8972.
33. Creighton, T. E. (1983) *Biopolymers 22*, 49−58.
34. Goldenberg, D. P. (1985) *J. Cell. Biochem. 29*, 321−335.
35. Lin, T. Y., and Kim, P. S. (1989) *Biochemistry 28*, 5282−5287.
36. Zhang, R., and Snyder, G. H. (1989) *J. Biol. Chem. 264*, 18472−18479.
37. Darby, N. J., and Creighton, T. E. (1993) *J. Mol. Biol. 232*, 873−896.
38. Dadlez, M., and Kim, P. S. (1996) *Biochemistry 35*, 16153−16164.
39. Jacobson, H., and Stockmayer, W. H. (1950) *J. Chem. Phys. 18*, 1600−1606.
40. Chan, H. S., and Dill, K. A. (1990) *J. Chem. Phys. 92*, 3118−3135.
41. Le-Nguyen, D., Heitz, A., Chiche, L., El Hajji, M., and Castro, B. (1993) *Protein Sci. 2*, 165−174.
42. Chang, J. Y., Canals, F., Schindler, P., Querol, E., and Avilés, F. X. (1994) *J. Biol. Chem. 269*, 22087−22094.
43. Schellman, J. A. (1955) *Compt. Rend. Lab. Carlsberg, Ser. Chim. 29*, 230−259.
44. Flory, P. J. (1956) *J. Am. Chem. Soc. 78*, 5222−5235.
45. Sosnick, T. R., Mayne, L., and Englander, S. W. (1996) *Proteins 24*, 413−426.
46. Baker, D. (2000) *Nature 405*, 39−42.
47. Mirny, L., and Shakhnovich, E. (2001) *Annu. Rev. Biophys. Biomol. Struct. 30*, 361−396.
48. Shea, J. E. and Brooks, R. C. L. (2001) *Annu. Rev. Phys. Chem. 52*, 499−535.
49. Plaxco, K. W., Simons, K. T., and Baker, D. (1998) *J. Mol. Biol. 277*, 985−994.
50. Goldenberg, D. P. (1999) *Nat. Struct. Biol. 6*, 987−990.
51. Fersht, A. R. (2000) *Proc. Natl. Acad. Sci. U.S.A. 97*, 1525−1529.
52. Itzhaki, L. S., Otzen, D. E., and Fersht, A. R. (1995) *J. Mol. Biol. 254*, 260−288.
53. Vendurscolo, M., Paci, E., Dobson, C. M., and Karplus, M. (2001) *Nature 409*, 641−645.
54. Kraulis, P. J. (1991) *J. App. Crystal. 24*, 946−950.
55. Merritt, E. A., and Bacon, D. J. (1997) *Methods Enzymol. 277*, 505−524.
56. Wu, J., Gage, D. A., and Watson, J. T. (1996) *Anal. Biochem. 235*, 161−174.

BI012033C